

## A PROXIMITY MEASURE USING BLINK MODEL

HAIFENG QIAN\*, HUI WAN\*, MARK N. WEGMAN\*, LUIS A. LASTRAS\*, AND RUCHIR PURI\*

**Abstract.** This paper proposes a new graph proximity measure. This measure is a derivative of network reliability. By analyzing its properties and comparing it against other proximity measures through graph examples, we demonstrate that it is more consistent with human intuition than competitors. A new deterministic algorithm is developed to approximate this measure with practical complexity. Empirical evaluation by two link prediction benchmarks, one in coauthorship networks and one in Wikipedia, shows promising results. For example, a single parameterization of this measure achieves accuracies that are 14–35% above the best accuracy for each graph of all predictors reported in the 2007 Liben-Nowell and Kleinberg survey.

**1. Introduction.** Humans have intuitions for graph proximity. Given a graph, certain pairs of nodes are perceived to have stronger relation strength than others. We know that a larger number of shorter paths indicate greater proximity, yet a precise mathematical formulation of such perception is elusive. Many measures in the literature can be viewed as quantitative proxies of graph proximity: shortest path, Jaccard index [19], Katz [23], personalized PageRank [33], SimRank [20], Adamic/Adar [2] and others [5, 6, 9, 16, 26–28, 31, 35, 40, 44]. Although they each have characteristics that suit specific applications, they generally have varying degrees of agreement with human intuition.

This manuscript adds one more entry to the list. This graph proximity measure is called the Blink Model and is a derivative of network reliability. By studying its properties and a series of graph examples, we argue that it matches human intuition better than many existing measures. We develop a practical algorithm to approximately compute this measure, and demonstrate its predicting power through empirical validations. Some of the contents appeared in [37].

Relational data, or graph-structured data, are ubiquitous. Graph proximity measures, i.e., the ability to quantify relation strength, are fundamental building blocks in many applications. They can be used to recommend new contacts in social networks [29], to make product recommendations based on a graph model of products and users [3], to rank web search results or documents in general [33], or to predict new facts in knowledge graphs [32]. They can be used to single out anomalies by identifying implausible links. The list of applications goes on and on.

The proposed measure is a derivative of terminal network reliability [4], which has other forms in various fields to be reviewed in Section 1.3. Network reliability has largely been ignored as a candidate measure in the aforementioned applications. For example, [35] concluded that network reliability was one of the least predictive measures. We prove the opposite conclusion with our Blink Model measure by including the winning measure from [35] in both theoretical and empirical comparisons. The discrepancy may be due to that [35] used a Monte-Carlo approximation with only 50 samples which were not sufficient to reach accurate results, and running a sufficient number of samples might have been computationally infeasible.

Exact evaluation of the Blink Model measure has the same complexity as terminal network reliability, which is known to be  $\#P$ -complete [41]. We will present a new deterministic algorithm that approximates the measure directly with practical complexity and thereby enables the proposed measure in applications.

---

\*IBM T. J. Watson Research Center, Yorktown Heights, New York ([qianhaifeng@us.ibm.com](mailto:qianhaifeng@us.ibm.com)).

To quantify the benefit of being consistent with human intuition, we use two link prediction tasks to compare our measure against other topological proximity measures. The first is a replication of [29]. A remarkable conclusion of [29] was that the best proximity measure is case dependent. A specific parameterization of a specific measure may perform well on one graph yet underperform significantly on another, and there does not exist a consistent winner. We compare against the oracle, i.e. the highest accuracy for each graph of all predictors in [29], and demonstrate that a single parameterization of our measure outperforms the oracle by 14–35% on each graph. The second task is predicting additions of inter-wikipedia citations in Wikipedia from April 2014 to March 2015, and again substantial accuracy advantage is shown. Through these tasks, we also demonstrate a simple yet practical and automatic method of training graph weighting parameters, which can naturally incorporate application-specific domain knowledge.

This manuscript is organized as follows. The rest of this section defines the problem, the proposed proximity measure and several competing measures, and reviews related fields and basic arithmetic. Section 2 studies properties of the measure and compares it with others through graph examples. Section 3 describes the proposed approximation algorithm. Section 4 presents empirical comparisons.

**1.1. Problem statement.** The problem statement for a proximity measure is the following. The input is a graph  $G = \langle V, E \rangle$ , its node weights  $w_V : V \rightarrow (0, 1]$ , and its edge weights  $w_E : E \rightarrow (0, 1]$ . The output is, for any pair of nodes A and B in  $V$ , a value score  $s(A, B)$ .

Note that not all proximity measures consider  $w_V$  and  $w_E$ . Some use  $w_E$  and ignore  $w_V$ , while some consider only topology  $G$ . Although  $w_V$  and  $w_E$  can be from any source, we present a simple yet practical method in Section 2.4 to train a few parameters and thereby set  $w_V$  and  $w_E$ . It's applicable to all proximity measures and is used in Section 4.

We will focus on directed simple edges. Undirected edges can be represented by two directed edges, and most discussions are extendable to hyperedges.

**1.2. Definitions.** Let us first define the proposed graph proximity measure. Consider the input  $G$  as a graph that blinks: an edge exists with a probability equal to its weight; a node exists with a probability equal to its weight. Edges and nodes each blink independently. A path is considered existent if and only if all edges and all intermediate nodes on it exist; note that we do not require the two end nodes to exist. The proposed proximity measure is

$$s(A, B) = -\log(1 - b(A, B)) \quad (1.1)$$

$$\text{where } b(A, B) = P[\text{at least one path exists from } A \text{ to } B] \quad (1.2)$$

We will refer to (1.1) as the Blink Model measure, its properties and generalizations to be presented in Section 2. It is straightforward to see that  $s$  and  $b$  are monotonic functions of each other and hence order equivalent, and the reason to choose  $s$  over  $b$  will be evident in Section 2.1.

Next we define several competing measures. For brevity, SimRank [20] and commute-time [16] are omitted and they are compared in Section 2.3.

Personalized PageRank (PPR) [33] with weights considers a Markov chain that has the topology of  $G$  plus a set of edges from each node to node A. These additional edges all have transition probability of  $\alpha \in (0, 1)$ . For each original edge  $e \in E$ , let X be its source node, let  $w_{\text{sum}, X}$  be the sum of weights of X's out-going edges,

and the transition probability of edge  $e$  is  $(1 - \alpha) \cdot w_E(e) / w_{\text{sum},X}$ . The PPR measure  $\text{score}_{\text{PPR}}(A, B)$  is defined as this Markov chain's stationary distribution on node B. PPR does not use node weights.

The original Katz measure [23] does not use edge or node weights, and we define a modified Katz measure:

$$\text{score}_{\text{Katz}}(A, B) = \sum_{l=1}^{\infty} \beta^l \cdot \sum_{\text{length-}l \text{ A-to-B path } i} p_{i,l} \quad (1.3)$$

where  $\beta \in (0, 1)$  is a parameter, and  $p_{i,l}$  is the product of edge weights and intermediate node weights for the  $i^{\text{th}}$  path with length  $l$ . This measure is divergent if  $\beta$  is larger than the reciprocal of the spectral radius of the following matrix  $M$ : entry  $M_{i,j}$  is the product of the  $i^{\text{th}}$  node weight and the sum of edge weights from the  $i^{\text{th}}$  node to the  $j^{\text{th}}$  node.

The effective conductance (EC) measure is defined as the effective conductance between two nodes by viewing edges as resistors. It can be generalized to be a directed measure, and notable variants include cycle-free effective conductance (CFEC) [26] and EC with universal sink [14, 40].

Expected Reliable Distance (ERD) is the winning measure in [35]. Consider the same blinking graph as in the Blink Model and let  $D$  be the shortest-path distance from A to B, ERD is an inverse-proximity measure:

$$\text{score}_{\text{ERD}}(A, B) = E[D | D \neq \infty] \quad (1.4)$$

Our implementation of Adamic/Adar [2] is:

$$\text{score}_{\text{AA}}(A, B) = \sum_C \frac{n_{A,C} \cdot n_{C,B}}{\log d_{C,\text{in}} + \log d_{C,\text{out}}} \quad (1.5)$$

where  $n_{A,C}$  is the number of A-to-C edges,  $n_{C,B}$  is the number of C-to-B edges, and  $d_{C,\text{in}}$  and  $d_{C,\text{out}}$  are the numbers of in-coming and out-going edges of node C.

**1.3. Related work.** This section briefly reviews fields related to the proposed measure.

Network reliability is an area in operations research which focuses on evaluating two-terminal reliability, i.e. (1.2), all-terminal reliability and other similar quantities. Target applications were assessing the reliability of ARPANET, tactical radio networks, etc. Complexity of exact evaluation of (1.2) was proved to be  $\#P$ -complete [41]. Fast exact methods were developed for special topologies [34, 39]. Deterministic methods were developed for evaluating bounds [4, 8]. Monte Carlo methods were developed for estimation [15, 22, 42], and were considered the choice for larger graphs with general topologies [4]. Most of these methods have poor scalability to large graphs. In a work [18] in 2007, which was a modern implementation based on binary decision diagrams (BDD), the largest square-2D-grid benchmark had only 144 nodes. In another work [38] in 2005, which used a Monte Carlo method, the largest benchmark had only 11 nodes.

Our blinking graph definition belongs to the category of random graphs [13, 17]. It is a generalization of the Edgar Gilbert model by having a different probability for each edge (zero probabilities remove edges from the Edgar Gilbert model). In particular, the branch of percolation theory [7, 25] and works on uncertain graphs [21, 35, 45, 46] are closely related to our study.

Network influence studies the spread of influence through social networks. A popular model, called independent cascade model [24], considers the same blinking graph with all node weights being 1, and the influence  $\sigma(S)$  is, given a set of starting nodes  $S$ , the expected number of reachable nodes from  $S$ . In the case of  $S = \{A\}$ ,  $\sigma(S)$  is equal to the sum of (1.2) over all node B's. The goal of optimization is to select  $S$  to maximize  $\sigma(S)$ . Since the quantity of interest is sum of (1.2) values, it is easier to compute than individual (1.2) values. For example, many fewer Monte Carlo samples are needed to reach the same relative error. Methods have been developed to quickly estimate  $\sigma(S)$  [10, 43], e.g., [43] uses the largest-probability single path to each node as a surrogate for an individual (1.2) value. Although these methods showed fidelity at the  $\sigma(S)$  level, they incur too much error for our purpose.

**1.4. Basic arithmetic.** For clarity of presentation and without loss of generality<sup>1</sup>, this section assumes all node weights being 1.

Exact evaluation of the Blink Model can be as follows. Enumerate all subgraphs of  $G$ , each of which is a state of the blinking graph and has a probability that is equal to the product of  $w_E(e)$  for edges  $e$  that exist and  $1 - w_E(e)$  for edges  $e$  that do not. (1.2) is the sum of probabilities of subgraphs where a path exists from A to B, and (1.1) gets calculated accordingly. This has impractical complexity.

Monte Carlo evaluation of the Blink Model measure can be as follows. Each sample traverses the subgraph reachable from A in one instance of the blinking graph. (1.2) is approximated by the fraction of samples that reach B, and (1.1) gets approximated accordingly. This can be expensive. In Table 3.1, we demonstrate that at least tens of thousands of samples are needed to reliably discern different pairs of nodes. Yet in Section 4.2 for a graph that represents Wikipedia citation network, practical run time allows only 100 samples.

If edges  $e_1 = (X, Y)$  and  $e_2 = (Y, Z)$  are the only edges to/from node Y, they can be replaced by a single edge from X to Z with weight  $w_E(e_1) \cdot w_E(e_2)$ , without altering the Blink Model measure for any pair of nodes.

Two parallel edges  $e_1$  and  $e_2$  can be replaced by a single edge with weight  $1 - (1 - w_E(e_1)) \cdot (1 - w_E(e_2))$ , without altering the Blink Model measure for any pair of nodes.  $x$  parallel edges with weight  $w$  is equivalent to a single edge with weight  $1 - (1 - w)^x$ . In other words, an edge with weight  $1 - (1 - w)^x$  is  $x$  times as strong as an edge with weight  $w$ .

**2. The Measure.** This section starts with two important properties of the proposed proximity measure, followed by its generalizations and variations. We then use a series of graph studies to demonstrate that the proposed measure is more consistent with human intuition than competitors, and finally discuss setting edge and node weights in applications.

**2.1. Properties.** Let us begin with two properties of (1.1), *additivity* and *monotonicity*, which are important in the coming sections.

*Additivity.* Let  $G_1 = \langle V_1, E_1 \rangle$  and  $G_2 = \langle V_2, E_2 \rangle$  be two graphs such that  $V_1 \cap V_2 = \{A, B\}$ ,  $E_1 \cap E_2 = \emptyset$ . Let  $G_3 = \langle V_1 \cup V_2, E_1 \cup E_2 \rangle$  be a combined graph that has the same node and edge weights as in  $G_1$  and  $G_2$ . Let  $s_{G_1}(A, B)$ ,  $s_{G_2}(A, B)$  and  $s_{G_3}(A, B)$  be

---

<sup>1</sup>Blinking graphs with edge weights alone, setting all node weights to 1, are equally expressive. A node weight can be expressed as an edge weight by splitting a node into two nodes, one being sink of in-coming edges, one being source of out-going edges, and adding an auxiliary edge between the two, with edge weight equal to the original node weight [4].

the measure value (1.1) in these three graphs respectively. Then this condition holds:

$$s_{G_3}(A, B) = s_{G_1}(A, B) + s_{G_2}(A, B) \quad (2.1)$$

Among competitors defined in Section 1.2, Adamic/Adar and EC have the same additivity property. Katz does not have this property, as in general (1.3) in  $G_3$  is more than the sum of that in  $G_1$  and  $G_2$ , and may even be divergent.

The additivity property is consistent with human intuition. When multiple independent sets of evidence are combined, our perception of proximity becomes the sum of proximity values derived from each individual set. To state the same in more general terms, the proposed proximity measure (1.1) is proportional to the amount of evidence, which is why we choose it over (1.2). This additivity is also crucial to the development of the approximation algorithm in Section 3.

*Monotonicity.* Let  $G_1 = \langle V_1, E_1 \rangle$  and  $G_2 = \langle V_2, E_2 \rangle$  be two graphs such that  $V_1 \subseteq V_2$ ,  $E_1 \subseteq E_2$ , and that their weights satisfy that  $w_{V_1}(X) \leq w_{V_2}(X), \forall X \in V_1$  and that  $w_{E_1}(e) \leq w_{E_2}(e), \forall e \in E_1$ . Let  $s_{G_1}(A, B)$  and  $s_{G_2}(A, B)$  be the measure value (1.1) in these two graphs respectively. Then the following condition holds.

$$s_{G_1}(A, B) \leq s_{G_2}(A, B), \forall A, B \in V_1 \quad (2.2)$$

In plain language, if an edge is added to a graph or if a node/edge weight is increased in a graph, then the proposed measure (1.1) will not decrease for any pair of nodes. This again is consistent with human intuition.

Among competitors defined in Section 1.2, Katz and EC have the same monotonicity property, assuming that the additional edges or added weights do not cause (1.3) to diverge. In Adamic/Adar's (1.5), if the denominator is viewed as reciprocal of  $w_V(C)$  which implies a specific choice<sup>2</sup> of  $w_V$ , then it also satisfies the monotonicity property. Note that (inverse) ERD is not monotonic because additional edges may form a new long path from A to B and hence increase (1.4).

**2.2. Generalizations.** The measure (1.1) is defined on a particular event, “a path exists from A to B”. This definition is a pair-wise proximity measure and is useful in for example link-prediction applications. For other applications, the definition (1.1) can be generalized to other events in the blinking graph: e.g., for a set of nodes  $S_A$  and another set of nodes  $S_B$ ,

$$\tilde{s}(S_A, S_B) = -\log(1 - P[\text{a path exists from any of } S_A \text{ to each of } S_B]) \quad (2.3)$$

Or for three nodes A, B and C,

$$\tilde{\tilde{s}}(A, B, C) = -\log(1 - P[\text{a path exists from A to B but no path exists from A to C}]) \quad (2.4)$$

And there are many more possibilities. In particular, when edges are labeled to indicate types of relations [32], the choice of event can involve edge labels.

The measure (1.1) is a proximity measure. Another variation is a distance measure:

$$d(A, B) = -\log(b(A, B)) \quad (2.5)$$

---

<sup>2</sup>Such choice of weights is shown to be beneficial in social networks [2]. With Blink Model, this can easily be encoded as domain knowledge, to be described in Section 2.4. In fact similar schemes are used in Section 4.

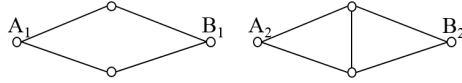


Fig. 2.1: A pair of graph examples.

It is straightforward to verify that the above definition satisfies the triangle inequality. It also has the monotonicity property. It has an additivity property that differs from that in Section 2.1, but is defined on two graphs in series.

**2.3. Graph studies.** This section uses graph examples to compare the proposed proximity measure with competitors to demonstrate that it is more consistent with human intuition. Comparison with Adamic/Adar (1.5) or common-neighbor (replacing the sum in (1.5) by a sum of 1's) is straightforward since they are limited to length-2 paths, and an example is omitted.

In examples in Figures 2.1–2.3, we argue that human intuition would say that node A has stronger relation to node B<sub>2</sub> than to B<sub>1</sub>. A key notion is that human intuition not only prefers more and shorter paths, but also prefers structures that are mutually corroborated. If an edge or path has no corroboration, its existence in the graph may be a random coincidence and hence does not indicate strong proximity. On the flip side, proximity is strong for an aggregate structure that is impervious to edges randomly existing.

In discussing all examples, we assume uniform node weights of 1 and uniform edge weights of  $w < 1$ .

Let us begin with Figure 2.1 of two undirected graphs. It could be perceived that there are two random paths from A<sub>1</sub> to B<sub>1</sub>, while the two length-2 paths from A<sub>2</sub> to B<sub>2</sub> are less likely to be random because the crossing edge provides mutual corroboration between them, and therefore human intuition prefers (A<sub>2</sub>, B<sub>2</sub>) over (A<sub>1</sub>, B<sub>1</sub>). Table 2.1 lists various proximity scores, where none is consistent with human intuition. Shortest-path and EC conclude that (A<sub>1</sub>, B<sub>1</sub>) and (A<sub>2</sub>, B<sub>2</sub>) are equally related, while CFEC [26] and commute-time [16] conclude that (A<sub>1</sub>, B<sub>1</sub>) is stronger than (A<sub>2</sub>, B<sub>2</sub>). In contrast, the Blink Model score is  $-2 \cdot \log(1 - w^2)$  for (A<sub>1</sub>, B<sub>1</sub>) and  $-\log(1 - 2w^2 - 2w^3 + 5w^4 - 2w^5)$  for (A<sub>2</sub>, B<sub>2</sub>), and the latter is strictly larger than the former. This shows a weakness of EC in that it sees no effect from the crossing edge in the second graph; the EC variant of CFEC [26] exacerbates this trait; another EC variant [14, 40] adds a universal sink to the EC model, and it is straightforward to verify that it also ranks (A<sub>1</sub>, B<sub>1</sub>) as stronger than (A<sub>2</sub>, B<sub>2</sub>), and similar effects of the universal sink have been reported in [26]. A spectrum of measures was proposed in [44], where shortest-path is one end of the spectrum while commute-time is the other end; although we are unable to judge intermediate variants of [44], Table 2.1 suggests that both of its corner variants produce counterintuitive rankings for Figure 2.1.

Next let us consider Figure 2.2(i). There are two equal-length paths from A to B<sub>1</sub> and to B<sub>2</sub>, but there are more paths going from A to B<sub>2</sub>. So it seems there's more reason to believe that it's not a coincidence that B<sub>2</sub> is connected to A than B<sub>1</sub>. PageRank scores are  $\text{score}_{\text{PPR}}(A, B_1) = (1 - \alpha)^2 / 2$  and  $\text{score}_{\text{PPR}}(A, B_2) = (1 - \alpha)^2 / 4$ . In other words, PPR considers that A has greater proximity to B<sub>1</sub> than to B<sub>2</sub>, and this holds true for any parameterization. In contrast, the Blink Model score (1.1) is higher for B<sub>2</sub> than B<sub>1</sub>.

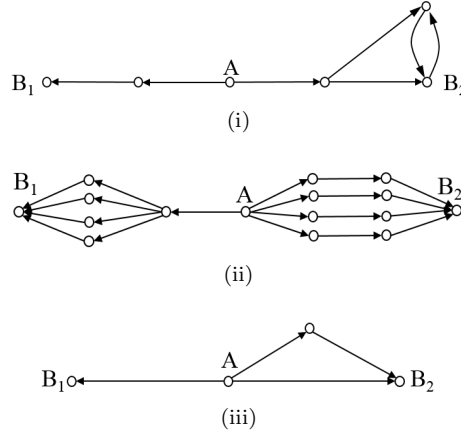


Fig. 2.2: Graph examples for PPR, Katz and ERD.

Table 2.1: Some proximity measures on Figure 2.1.

Measure	$A_1, B_1$	$A_2, B_2$
1/shortest-path	$1/(2w)$	$1/(2w)$
1/commute-time	$1/(8w)$	$1/(10w)$
EC	$w$	$w$
CFEC	$w$	$8w/9$

Consider the Katz measure (1.3) on Figure 2.2(ii). It's straightforward to verify that, with any  $w$  and  $\beta$  values, we have  $\text{score}_{\text{Katz}}(A, B_1) = \text{score}_{\text{Katz}}(A, B_2)$ , including when  $w$  is 1 and (1.3) becomes the original Katz. In other words, the (modified) Katz measure cannot discern  $B_1$  and  $B_2$  relative to  $A$ , because it sees no difference between the four paths to  $B_1$  and those to  $B_2$ . In contrast, the Blink Model measure (1.1) recognizes that the edge to the left of  $A$ , which all paths to  $B_1$  depend on, has no corroboration, and we have  $s(A, B_1) < s(A, B_2)$ , consistent with human intuition.

Next consider the ERD measure (1.4) on Figure 2.2(iii), and we have  $\text{score}_{\text{ERD}}(A, B_1) = 1$  and  $\text{score}_{\text{ERD}}(A, B_2) > 1$ . Since ERD is an inverse proximity, the conclusion is that  $A$  has greater proximity to  $B_1$  than to  $B_2$ , and is inconsistent with human intuition. Blink Model shows the reverse.

Next consider SimRank [20] on a three-node undirected complete graph and on a four-node undirected complete graph. It is straightforward to verify that the SimRank score, under any parameterization, is higher for a pair of nodes in the former than in the latter, and in fact the score always decreases as the size of a complete graph increases. This is contrary to our Blink Model and human intuition. To be fair, SimRank was designed as a similarity measure and was not intended to be a proximity measure. This is also the likely reason that its performance in [29] was reported to be mediocre.

The last example graph is Figure 2.3, which demonstrates the advantage of measure (1.1) over a class of methods. Continuing the intuition from Figure 2.1, on the left there exists mutual corroboration between the top pair of length-3 paths to  $B_1$  and between the bottom pair of length-3 paths, but none exists between the two pairs.

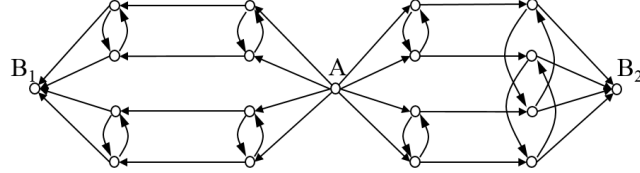


Fig. 2.3: A graph example.

On the right there exists mutual corroboration among all four length-3 paths to  $B_2$ , and the proximity to  $B_2$  is perceived as more robust to a human. This is analogous to using four strings to reinforce four poles, and a human is more likely to use a pattern similar to the right half of Figure 2.3 than the left. The Blink Model recognizes that  $B_2$  is more connected to  $A$  than  $B_1$ , e.g. when  $w$  is 0.5,  $s(A, B_1) = 0.795$  and  $s(A, B_2) = 0.809$ .

Consider any algorithm which operates on local storage per node: it starts with special storage in source node  $A$ , all other nodes starting equal; on each successive iteration, it updates information stored in each node based on information stored in adjacent nodes from the previous iteration. Such an algorithm can easily for example compute shortest-path distance from  $A$ , the PPR score, the Katz score, and the EC score. However, such an algorithm, even with an infinite amount of storage and an infinite number of iterations, cannot distinguish  $B_1$  and  $B_2$  in Figure 2.3; in fact, the eight nodes that are distance-2 from  $A$  are also indistinguishable. Algorithms of this type encompass a large range of methods. In particular, any matrix computation based on the adjacency matrix or variants of the adjacency matrix, which includes almost all measures that have a random-walk-based definition, falls into this category, and no possible linear algebra can determine that  $B_2$  is closer than  $B_1$ . This is a blessing and a curse: the Blink Model can discern cases correctly, but is inherently hard to compute.

**2.4. Training weights.** This section addresses a practical issue of using the Blink Model in an application: how to set edge and node weights. There are many ways, and we describe a simple yet practical method to do so by training a few parameters.

Let two functions  $f_E : E \rightarrow R_{>0}$  and  $f_V : V \rightarrow R_{>0}$  represent domain knowledge. In applications where we have no domain knowledge beyond the topology  $G$ , we simply have  $f_E$  and  $f_V$  equal to 1 for all. In applications where we do, we assume that  $f_E$  and  $f_V$  are larger for more important or more reliable edges and nodes, and that their values exhibit linearity: two parallel edges  $e_1$  and  $e_2$  can be replaced by a single edge  $e_3$  with  $f_E(e_3) = f_E(e_1) + f_E(e_2)$ .

Our method sets graph edge and node weights as:

$$\begin{aligned} w_E(e) &= 1 - (1 - b_1)^{f_E(e)}, \forall e \in E \\ w_V(v) &= 1 - (1 - b_2)^{f_V(v)}, \forall v \in V \end{aligned} \tag{2.6}$$

where  $b_1, b_2 \in (0, 1)$  are two tunable parameters<sup>3</sup>. It is straightforward to verify that the linearity assumption on  $f_E$  is consistent with the arithmetic in Section 1.4.

<sup>3</sup>One way to interpret  $b_1$  and  $b_2$ , or  $w_E$  and  $w_V$  in general, is that they encode varying personalities, while the analysis engine (1.1) is invariant. This is similar to that different people, when

Parameters  $b_1$  and  $b_2$  for Blink Model are similar to  $\alpha$  for PageRank and  $\beta$  for Katz, and we search for best values by using training data in an application. If  $f_E$  and  $f_V$  have tunable parameters, those can be trained in the same process. Since we introduce only two parameters, the training process is straightforward and can be brute-force scan and/or greedy search.

This method is applicable to all proximity measures and is used for all in Section 4. One caveat is that certain measures work better with linear weights:

$$\begin{aligned} w_E(e) &= b_1 \cdot f_E(e), \forall e \in E \\ w_V(v) &= b_2 \cdot f_V(v), \forall v \in V \end{aligned} \quad (2.7)$$

For example, we observe empirically that PPR works better with (2.7), which is intuitive given the linearity assumption on  $f_E$ , while Modified Katz and ERD prefer (2.6). Note that when  $b_1$  and  $b_2$  are small, (2.6) asymptotically becomes (2.7).

**3. Approximation Algorithm.** We present a deterministic algorithm that approximates (1.1) directly. Without loss of generality (per Section 1.4), we describe this algorithm under the conditions of all node weights being 1 and that  $G$  is a simple directed graph where parallel edges are already merged.

**3.1. Overall flow.** A *minimal path* from node A to node B is defined as a path from A to B without repeating nodes. For a finite graph  $G$ , there exist a finite number of minimal paths. Consider a single minimal path  $i$  from node A to node B. We define the following<sup>4</sup> as the *nominal contribution* of this path to (1.1).

$$s_{\text{path } i} = -\log \left( 1 - \prod_{\text{edge } e \text{ on path } i} w_E(e) \right) \quad (3.1)$$

By the additivity property (2.1), if all minimal paths from A to B are mutually disjoint, we can compute (1.1) exactly by summing (3.1) over all minimal paths. Of course this is not true for general graphs where paths from A to B overlap each other and (1.1) is less than the sum of  $s_{\text{path } i}$  values.

However, if we consider only length-1 and length-2 minimal paths, they can never share an edge with each other, and their nominal contributions can be added according to the additivity property. Further invoking the monotonicity property (2.2), we obtain the following inequality.

$$\sum_{\text{path } i \text{ with length 1 or 2}} s_{\text{path } i} \leq s(A, B) \leq \sum_{\text{path } i} s_{\text{path } i} \quad (3.2)$$

Therefore, the key to approximate (1.1) is to quantify the contribution of minimal paths that are longer than 2.

We start the approximation by making the following conjecture that the contribution of each minimal path  $i$  is quantifiable as a value  $\hat{s}_{\text{path } i}$  such that  $s(A, B) =$

presented with the same evidence, may make different decisions. In Section 4 for example, we scan for  $b_1$  and  $b_2$  that match the collective behavior of physicists or Wikipedia contributors.

<sup>4</sup>We omit A and B from  $s_{\text{path } i}$  and  $\hat{s}_{\text{path } i}$  notations to keep formulas concise. Note that any path refers to a minimal path in  $G$  from A to B.

$\sum_{\text{path } i} \hat{s}_{\text{path } i}$ . We use  $G'$  to denote a subgraph of  $G$  and  $s_{G'}(A, B)$  to denote the measure value (1.1) in  $G'$ .

**CONJECTURE 1.** *A value  $\hat{s}_{\text{path } i}$  exists for each minimal path  $i$  from node  $A$  to node  $B$ , such that these  $\hat{s}_{\text{path } i}$  values satisfy the following conditions:*

$$\begin{aligned} \hat{s}_{\text{path } i} &= s_{\text{path } i}, \text{ if path } i \text{ has length 1 or 2} \\ 0 \leq \hat{s}_{\text{path } i} &\leq s_{\text{path } i}, \text{ if path } i \text{ is longer than 2} \end{aligned} \quad (3.3)$$

$$\begin{aligned} s_{G'}(A, B) &\geq \sum_{\substack{\text{path } i \text{ is contained in } G'}} \hat{s}_{\text{path } i} \\ s_{G'}(A, B) &\leq \sum_{\substack{\text{path } i \text{ overlaps with } G'}} \hat{s}_{\text{path } i} \end{aligned} \quad (3.4)$$

for any subgraph  $G'$ .

Our algorithm works best when Conjecture 1 holds, while the approximation would be coarser when it does not. We have not found any graph that breaks Conjecture 1, and it remains unproven whether it holds for all graphs. We use Conjecture 1 in two ways. By selecting a special set of subgraphs  $G'$ , we utilize (3.4) to iteratively approximate  $\hat{s}_{\text{path } i}$  values. Then, after obtaining approximate  $\hat{s}_{\text{path } i}$  values, we invoke Conjecture 1 for a special case of  $G' = G$ , where the two sums in condition (3.4) are identical and therefore (3.4) becomes two equalities. This justifies that  $s(A, B) = \sum_{\text{path } i} \hat{s}_{\text{path } i}$  which achieves our purpose.

One observation is that Conjecture 1 does not uniquely define  $\hat{s}_{\text{path } i}$  values as there may exist two sets of  $\hat{s}_{\text{path } i}$  values that both satisfy (3.3)(3.4). However, by definition they both sum up to the same end result (1.1), and therefore we only need to find one such set of  $\hat{s}_{\text{path } i}$  values. A second observation is that the lower bound in (3.4) is tight for a variety of subgraphs  $G'$ , while the upper bound is tight only for large subgraphs. We exploit this observation in the proposed algorithm: we will select/design a certain set of subgraphs  $G'$  where the lower bound in (3.4) is tight, and then use the lower bound as an equality to iteratively refine the approximated  $\hat{s}_{\text{path } i}$  values.

The proposed algorithm is illustrated in Algorithm 1.  $\hat{s}_{\text{path } i}$  values are initialized to be the nominal. A subgraph  $G'_i$ , to be elaborated later, is selected for each path  $i$  longer than 2, and  $s_{G'_i}(A, B)$  is computed/approximated. During each iteration, for each path  $i$  longer than 2, we use the lower bound in (3.4) as an equality and convert it to the following update formula.

$$\hat{s}_{\text{path } i}^{k+1} = \frac{\hat{s}_{\text{path } i}^k \cdot \left( s_{G'_i}(A, B) - \sum_{\text{path } j \in \Upsilon_i} s_{\text{path } j} \right)}{\sum_{\text{path } j \in \Xi_i} \hat{s}_{\text{path } j}^k} \quad (3.5)$$

where  $k$  is the iteration index,  $\Xi_i$  is the set of minimal paths from  $A$  to  $B$  that are contained in  $G'_i$  and that have length more than 2, and  $\Upsilon_i$  is the set of minimal paths from  $A$  to  $B$  that are contained in  $G'_i$  and that have length of 1 or 2.

**ALGORITHM 1.** *Overall flow of the proposed algorithm.*

---

```

 $\hat{s}_{\text{path } i}^0 \leftarrow s_{\text{path } i}, \forall \text{ path } i, \text{ using (3.1);}$ 
select subgraphs  $G'_i, \forall \text{ path } i \text{ longer than 2;}$ 
for  $k = 0, 1, \dots$ , until convergence:
  compute  $\hat{s}_{\text{path } i}^{k+1}$  using (3.5),  $\forall \text{ path } i \text{ longer than 2;}$ 
   $s(A, B) \leftarrow \text{sum of final } \hat{s}_{\text{path } i} \text{ values;}$ 

```

---

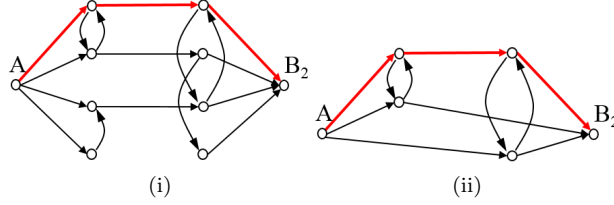


Fig. 3.1: (i) The selected subgraph of Figure 2.3 for the highlighted path, and (ii) its simplified form.

One way to interpret this algorithm is that it is an iterative solver that solves a linear system where there is one equation for each  $G'_i$  and the unknowns are  $\hat{s}_{\text{path } i}$ . This interpretation holds for the variation in Section 3.2, however it does not hold in Sections 3.3 and 3.4, in which we will present an alternative interpretation. In the next three sections, we present three variations of the proposed algorithm. They differ in how they select/construct subgraph  $G'_i$  for a given path  $i$ . Section 3.5 discusses selecting minimal paths to work on.

**3.2. High-accuracy variation.** In this variation of the proposed algorithm, we select subgraph  $G'_i$  as the minimal subgraph that contains all minimal paths from A to B which overlap with path  $i$  by at least one edge. One example is illustrated in Figure 3.1(i), which shows the subgraph of Figure 2.3 for the highlighted path from A to  $B_2$ , and it is used in (3.5) to update  $\hat{s}$  of the highlighted path during each iteration. Note that  $G'_i$  only needs to be identified once and  $s_{G'_i}(A, B)$  only needs to be evaluated once, and the same value is reused in (3.5) across iterations.

A main computation in this variation is the evaluation of  $s_{G'_i}(A, B)$ . Since  $G'_i$  is much smaller than the whole graph  $G$  in typical applications, many techniques from the network reliability field can be applied to approximately evaluate (1.2) in  $G'_i$  and hence  $s_{G'_i}(A, B)$ . For example, it is known that (1.2) is invariant under certain topological transformations [4, 39]. Applying such transformations, the graph in Figure 3.1(i) can be simplified to Figure 3.1(ii) without loss of accuracy. Then a Monte Carlo method can be applied on the simplified graph and approximate  $s_{G'_i}(A, B)$ .

**3.3. Medium-accuracy variation.** Instead of identifying and solving each  $G'_i$  as an actual subgraph, in this variation we construct  $G'_i$  as a hypothetical subgraph for each path  $i$  during each iteration.

We start the construction by considering the amount of sharing on each edge. In the  $k^{\text{th}}$  iteration, for edge  $e$ , define

$$u_e^k = \sum_{\text{path } j \text{ contains } e \text{ and is longer than 2}} \hat{s}_{\text{path } j}^k \quad (3.6)$$

Intuitively,  $u_e^k$  quantifies usage of edge  $e$  by A-to-B minimal paths, based on current knowledge at the  $k^{\text{th}}$  iteration.

For each path  $i$ , we annotate each edge on this path with  $u_e^k$ . Figure 3.2(i) illustrates a middle section of an example path  $i$ . We use  $u_{XY}^k$  to denote  $u_e^k$  when  $e$  is an edge from node X to node Y, and  $w_{XY}$  to denote its edge weight. Without loss of generality, we assume that  $u_{FG}^k > u_{CD}^k > u_{EF}^k > u_{DE}^k$ .

We construct the hypothetical subgraph  $G'_i$  starting from path  $i$  itself and by adding hypothetical edges. Since  $u_{EF}^k > u_{DE}^k$ , there must exist one or more A-to-B

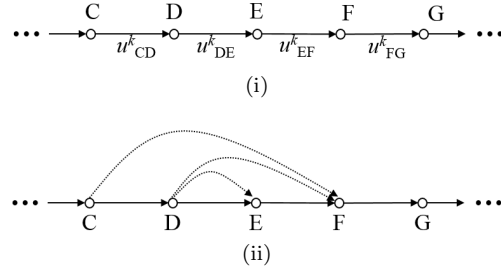


Fig. 3.2: (i) Example of a middle section of a path. (ii) The same middle section after adding hypothetical edges.

path(s) that passes the edge from E to F but that does not pass the edge from D to E. A hypothetical new edge from D to E is added to approximate the effect of such path(s); furthermore, we know that the sum of  $\hat{s}^k$  of these paths is equal to  $u_{EF}^k - u_{DE}^k$ , and we use this fact to assign the following weight.

$$w'_{DE} = 1 - (1 - w_{DE})^{(u_{EF}^k - u_{DE}^k)/u_{DE}^k} \quad (3.7)$$

In plain words, we assume that this hypothetical edge is  $(u_{EF}^k - u_{DE}^k) / u_{DE}^k$  times as strong as original D-to-E edge.

Similarly, since  $u_{CD}^k > u_{EF}^k$ , there must exist one or more A-to-B path(s) that passes the edge from C to D, but that does not pass the edge from E to F, the edge from D to E, or paths represented by the hypothetical edge from D to E. A hypothetical new edge from D to F is added to approximate the effect of such path(s). Again, we know that the sum of  $\hat{s}^k$  of these paths is equal to  $u_{CD}^k - u_{EF}^k$ , and by the same argument for (3.7), we assign the following edge weight.

$$w'_{DF} = 1 - \left(1 - w_{EF} \cdot \left(1 - (1 - w_{DE})^{u_{EF}^k / u_{DE}^k}\right)\right)^{\frac{u_{CD}^k - u_{EF}^k}{u_{EF}^k}} \quad (3.8)$$

The same rationale applies to adding the hypothetical edge from C to F, and so on.

The above construction process for  $G'_i$  processes edges on path  $i$  one by one in the order of increasing  $u_e^k$  values and adds hypothetical edges. The last step of construction is to add to  $G'_i$  the length-2 A-to-B paths that overlap with path  $i$ , since they are not visible in  $u_e^k$  values. The completed hypothetical subgraph  $G'_i$  is then used in (3.5) to compute  $\hat{s}_{\text{path } i}^{k+1}$  for the next iteration, and the overall algorithm proceeds. Note that the denominator  $\sum_{\text{path } j \in \Xi_i} \hat{s}_{\text{path } j}^k$  in (3.5) is simply equal to the largest  $u_e^k$  along path  $i$ ; let it be  $u_{\max}^k$ .

One distinction between this variation and Section 3.2 is that the exact evaluation of  $s_{G'_i}(A, B)$  has linear complexity with respect to path length. The hypothetical edges form series-parallel structures that are friendly to topological transformations [34, 39]. Using Figure 3.2(ii) as an example, the hypothetical D-to-E edge and the original D-to-E edge can be merged into a single edge; then it and the E-to-F edge can be merged into a single D-to-F edge; then it and the hypothetical D-to-F edge can be merged, and so on.

Another distinction between this variation and Section 3.2 is that  $G'_i$  is no longer the same across iterations. As a result, the linear-system interpretation mentioned

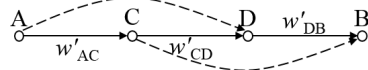


Fig. 3.3: Hypothetical subgraph in low-accuracy variation.

Table 3.1: Performance on Figure 2.3.  $\text{Error}_{B_2}$  and  $\text{Error}_\Delta$  are relative errors in  $s(A, B_2)$  and in  $s(A, B_2) - s(A, B_1)$ .

Edge weight	0.1			0.5			0.9		
	$\text{Error}_{B_2}$	$\text{Error}_\Delta$	Runtime(s)	$\text{Error}_{B_2}$	$\text{Error}_\Delta$	Runtime(s)	$\text{Error}_{B_2}$	$\text{Error}_\Delta$	Runtime(s)
High accuracy	0.07%	19.2%	7.68E-3	2.40%	12.4%	6.73E-3	2.40%	6.73%	7.74E-3
Medium accuracy	8.86%	100%	1.48E-3	17.2%	100%	1.50E-3	12.0%	100%	4.78E-4
MC, 1K samples	37.7%	4.21E2	9.53E-4	3.38%	282%	1.94E-3	43.1%	228%	2.09E-3
MC, 10K samples	12.9%	1.56E2	8.45E-3	1.07%	106%	1.84E-2	3.82%	272%	1.91E-2
MC, 100K samples	3.55%	4751%	8.27E-2	0.35%	29.2%	0.174	1.05%	70.2%	0.182
MC, 1M samples	1.13%	1852%	0.812	0.11%	8.69%	1.74	0.33%	23.7%	1.78

in Section 3.1 no longer holds. Instead, the following interpretation is more intuitive. The calculation by (3.5) applies a dilution factor  $\hat{s}_{\text{path } i}^k / u_{\max}^k$  on the strength of  $G'_i$  excluding length-2 paths. The more path  $i$  overlaps with other paths, the larger  $u_{\max}^k$  is and the smaller the dilution factor is, and  $G'_i$  is a hypothetical subgraph that mimics a path where every edge has usage  $u_{\max}^k$ .

**3.4. Low-accuracy variation.** Continuing the interpretation from the last section, we may construct  $G'_i$  in the form of Figure 3.3, which results in a tradeoff with further lower accuracy and lower runtime.

For minimal path  $i$ , let  $C$  and  $D$  be the first and last intermediate nodes, let the original edge weights along this path be  $w_1, w_2, \dots, w_n$ , and let edge usages (3.6) along this path be  $u_1^k, u_2^k, \dots, u_n^k$ . We construct a hypothetical subgraph  $G'_i$  in the form of Figure 3.3. In Figure 3.3, dashed arrows from  $A$  to  $D$  and from  $C$  to  $B$  represent edges that may exist in  $G$  and form length-2 paths  $A-D-B$  and  $A-C-B$ ; if these dashed edges do exist, they have their original weights. The weights of the three solid edges are:

$$w'_{AC} = 1 - (1 - w_1)^{u_{\max}^k / u_1^k} \quad (3.9)$$

$$w'_{CD} = 1 - \left(1 - \prod_{j=2}^{n-1} w_j\right)^{u_{\max}^k / u_{\text{mean}}^k} \quad (3.10)$$

$$w'_{DB} = 1 - (1 - w_n)^{u_{\max}^k / u_n^k} \quad (3.11)$$

where  $u_{\text{mean}}^k$  is a weighted average of  $u_2^k, \dots, u_{n-1}^k$ :

$$u_{\text{mean}}^k = \left( \sum_{j=2}^{n-1} u_j^k \cdot \log(w_j) \right) / \sum_{j=2}^{n-1} \log(w_j) \quad (3.12)$$

Intuitively,  $G'_i$  still mimics a path where every edge has usage  $u_{\max}^k$ , and is constructed more crudely than in Section 3.3.

**3.5. Accuracy and implementation issues.** This algorithm can discern  $B_1$  and  $B_2$  correctly for all cases in Section 2.3, and Table 3.1 shows details on Figure 2.3, with three cases where all edge weights are 0.1, 0.5 and 0.9 respectively. The medium-accuracy variation is unable to distinguish  $B_1$  and  $B_2$  and hence has 100% Error $_{\Delta}$ . Each Monte Carlo (MC) measurement is repeated with 100 different random number generation seeds, and the reported error/runtime is the average over the 100 runs. Not surprisingly, MC favors 0.5 edge weight and has larger errors for higher or lower weights, while our algorithm is stable across the range. Table 3.1 suggests that the high-accuracy variation has comparable accuracy to 10K MC samples for individual-score estimation, and is more accurate in differentiating  $B_1$  and  $B_2$  than one million samples for two of the three cases. It also suggests that a MC method needs at least tens of thousands of samples to reliably differentiate nodes.

For this graph, the high-accuracy runtime is equal to 3500–8000 MC samples, while the medium-accuracy runtime is equal to 200–1500 samples. In practice, different variations can form a hybrid: medium- or even low-accuracy variation is used for all target nodes and identifies a critical subset of targets, while high-accuracy variation only ranks within the critical subset.

With any variation, the input to the proposed algorithm is a set of minimal paths from  $A$  to  $B$ , and the output are  $\hat{s}$  values for each path in the set. For large graphs, to maintain practical complexity, the set is a subset of all minimal paths, and this results in underestimation of the Blink Model score (1.1). A natural strategy is to ignore long and weak paths, similar to [31] with respect to PageRank. This is motivated by the fact that the measure (1.2) has locality [22]. In our implementation, a minimal path  $i$  is given to the proposed algorithm if and only if it satisfies both of the following conditions:

$$s_{\text{path } i} \geq t_1 \quad (3.13)$$

$$\prod_{\text{edge } e \text{ on path } i} \frac{\log(1 - w_E(e))}{\sum_{\text{edge } f \in \Theta_e} \log(1 - w_E(f))} \geq t_2 \quad (3.14)$$

where  $\Theta_e$  is the set of out-going edges from the source node of  $e$ , and  $t_1$  and  $t_2$  are two constant thresholds that control runtime-accuracy tradeoff. Condition (3.14) is essentially a fan-out limit on paths. When making predictions in Section 4, we use  $t_2=2E-6$  which implies that we consider at most 500,000 paths from  $A$ .<sup>5</sup> For node  $B$  that is close to  $A$ , the above strategy provides good coverage of a “local” region and thus causes little underestimation. The further away  $B$  is from  $A$ , the less complete this coverage is and the more the underestimation is. In applications where we rank multiple  $B$  nodes for a given  $A$ , e.g. link prediction, fidelity is maintained because the degree of underestimation is negatively correlated with exact scores. For a distant node  $B$  where no path satisfies the bounds, we use a single path with the largest  $s_{\text{path } i}$ , which can be found efficiently with a Dijkstra’s-like procedure.

On a last note, our algorithm is essentially a method to quantify values for a set of uncertain and mutually overlapping pieces of evidence, each piece being a minimal path. The algorithm is orthogonal to the choice of input evidence, for which any path collection implementation can be used, while the quality of output is influenced by the quality of input.

<sup>5</sup>Identification of minimal paths to many  $B$ ’s can be achieved by a single graph traversal from  $A$ . For example, if the traversal finds a path composed of nodes  $A, B_1, B_2, \dots, B_n$ , which satisfy (3.13)(3.14), then this provides one qualified path to  $B_1$ , one to  $B_2$ ,  $\dots$ , and one to  $B_n$ .

**4. Experimental Results.** This section compares the predictive power of our method against competitors on two temporal link prediction tasks. Data and benchmarking code are released at [36]. All blink-model runs use the variation of Section 3.3; single-thread run time is 2.9–5.0 seconds per starting node in coauthorship graphs and 5.3 seconds in the Wikipedia graph, on a Linux server with Intel E7-8837 processors at 2.67GHz.

We use the method of Section 2.4 with two scenarios: graph #1 is with no domain knowledge,  $f_E$  and  $f_V$  being 1 for all, and hence with uniform edge and node weights  $b_1$  and  $b_2$ ; graph #2 is with domain knowledge expressed in  $f_E$  and  $f_V$ . In Section 4.1, we follow the practice of [29] and scan parameters for each predictor without separating training and test sets. In Section 4.2, we separate data into a training set and a test set, and the training set is used to scan for the best parameterization, while the test set is used for evaluation. Best parameter values for each predictor are listed in Tables 4.2 and 4.4; no-effect parameters are omitted, e.g., PPR scores are invariant with respect to  $b_1$  and  $b_2$ .

We focus on evaluating individual proximity measures and do not compare with ensemble methods [30]. We use structured input data as is, and do not utilize text of arXiv papers or Wikipedia pages. In real life applications, natural language processing (NLP) can be used to provide additional edges, edge labels and more meaningful edge weights [32], and thereby enhance prediction accuracy. Furthermore, such data from NLP are inherently noisy, which fits perfectly with the underlying philosophy of the Blink Model that any evidence is uncertain.

Table 4.1: Statistics of the coauthorship networks. Entry format is our-number/number-reported-in- [29]. Column Collaborations denotes pairwise relations in the training period. Column  $|E_{\text{old}}|$  denotes pairwise relations among Core authors in the training period. Column  $|E_{\text{new}}|$  denotes new pairwise relations among Core authors formed in the test period.

	Training Period			Core		
	Authors	Articles	Collaborations	Authors	$ E_{\text{old}} $	$ E_{\text{new}} $
astro-ph	5321/5343	5820/5816	41575/41852	1563/1561	6189/6178	5719/5751
cond-mat	5797/5469	6698/6700	23373/19881	1387/1253	2367/1899	1514/1150
gr-qc	2150/2122	3292/3287	5800/5724	484/486	523/519	397/400
hep-ph	5482/5414	10277/10254	47788/47806	1786/1790	6629/6654	3281/3294
hep-th	5295/5241	9497/9498	15963/15842	1434/1438	2316/2311	1569/1576

**4.1. Link prediction in arXiv.** This section replicates the experiments in [29] which are the following. For five areas in arXiv, given the coauthors of papers published in the training period 1994–1996, the task is to predict new pairwise coauthorship relations formed in the test period 1997–1999. Predictions are only scored for those within *Core* authors, defined as those who have at least 3 papers in the training period and at least 3 papers in the test period; this Core list is unknown to predictors. Table 4.1 gives statistics of the five graphs and prediction tasks. Let  $E_{\text{new}}$  be the set of new pairwise coauthorship relations among Core authors formed in the test period. Let  $E_p$  be the top  $|E_{\text{new}}|$  pairs among Core authors that are predicted by a predictor, and the score of this predictor is defined as  $|E_p \cap E_{\text{new}}|/|E_{\text{new}}|$ .

Table 4.1 shows that our setup matches [29] closely for four of the five benchmarks. We focus on benchmarks astro-ph, hep-ph and hep-th, for the following reasons. Benchmark cond-mat differs significantly from that reported in [29], thus is not

Table 4.2: Comparison of predictor accuracies on coauthorship networks.  $A$  denotes the accuracy score of a predictor.  $R$  denotes the ratio of  $A$  over that of oracle of [29].

	parameters	astro-ph		hep-ph		hep-th	
		$A$	$R$	$A$	$R$	$A$	$R$
Oracle of [29]	varying	8.55%		7.2036%		7.9407%	
Oracle of Blink, graph #1	varying	9.075%	1.061	8.3816%	1.164	8.8592%	1.116
Blink, graph #1	$b_1 = 0.5, b_2 = 0.4$	7.7461%	0.906	7.8025%	1.083	8.0306%	1.011
Blink, graph #2	$b_1 = 0.8, b_2 = 0.6, \gamma = 5$	10.264%	<b>1.200</b>	9.6922%	<b>1.345</b>	9.0504%	<b>1.140</b>
PPR, graph #2	$\alpha = 0.50$	8.5330%	0.998	6.7358%	0.935	7.9031%	0.995
Modified Katz, graph #2	$b_1 = 0.5, b_2 = 0.1, \beta = 0.1, \gamma = 5$	8.4106%	0.984	8.2292%	1.142	7.8394%	0.987
ERD, 10K samples, graph #1	$b_1 = 0.9, b_2 = 0.9$	8.4281%	0.986	8.1682%	1.134	7.1383%	0.899
ERD, 10K samples, graph #2	$b_1 = 0.9, b_2 = 0.9, \gamma = 4$	9.5471%	1.117	8.7473%	1.214	7.1383%	0.899

a valid benchmark to compare against the oracle of [29]. In gr-qc, 131 out of the 397 new relations were formed by a single project which resulted in three papers in the test period, with nearly identical 45-46 authors, [1] being one of the three. Because the size of gr-qc is not large enough relative to this single event, the scores of the predictors are distorted. Thus it is not a surprise that [29] reported that the best predictor for gr-qc is one that deletes 85-90% of edges as a preprocessing step, and that the same predictor delivers poor performance on the other benchmarks.

In Table 4.2, the oracle of [29] is the highest score for each benchmark, by all predictors including meta-approaches; note that no single predictor has such performance, and PPR and Katz on uniformly weighted graphs are dominated by the oracle. In graph #1, each paper is modeled by a hyperedge with uniform weight. Allowing the best  $b_1$  and  $b_2$  per graph leads to the oracle of Blink which easily beats the oracle of [29]; for a single parameterization, we get the next row where Blink wins two out of three. Such performance already puts Blink above all predictors reported in [29].

In graph #2, each paper is modeled as a node, and it connects to and from each of its authors with two directed simple edges. We provide domain knowledge through the following  $f_E$  and  $f_V$ . For an edge  $e = (X, Y)$ ,  $f_E(e) = 1 / \max(1, \log_\gamma d_X)$ , where  $d_X$  is the out degree of  $X$ . For a paper node, we set  $f_V$  to infinity and hence weight to 1. For an author node,  $f_V(\text{author}) = 1 / \max(1, \log_\gamma m_{\text{author}})$ , where  $m_{\text{author}}$  is the number of coauthors of this author in the training period.  $\gamma$  is a tunable parameter and is scanned with other parameters and reported in Table 4.2.

With graph #2, the predictor scores are asymmetric. For PPR and Katz, we experimented with max, min, sum and product of two directional scores, and the max gives the best results and is reported. For the Blink Model, we define symmetric score(A,B) =  $-\log(1 - b(A, B) \cdot b(B, A))$ . For ERD, the shortest-path distance in a Monte Carlo sample is defined as the shorter between the A-to-B path and the B-to-A path.

Table 4.2 demonstrates the proposed proximity measure's superior predictive power over competitors, as expected from discussions in Section 2, and a single parameterization of Blink Model outperforms oracle of [29] by 14–35%. Figure 4.1 shows receiver-operating-characteristic (ROC) curves. Blink with graph #2 clearly dominates the ROC curves. There is not a clear runner-up among the three competitors. Note that ERD #2 performs well on hep-ph for early guesses at around 5% true positive rate, but it degrades quickly after that and becomes the worst of the four by the 20% rate.

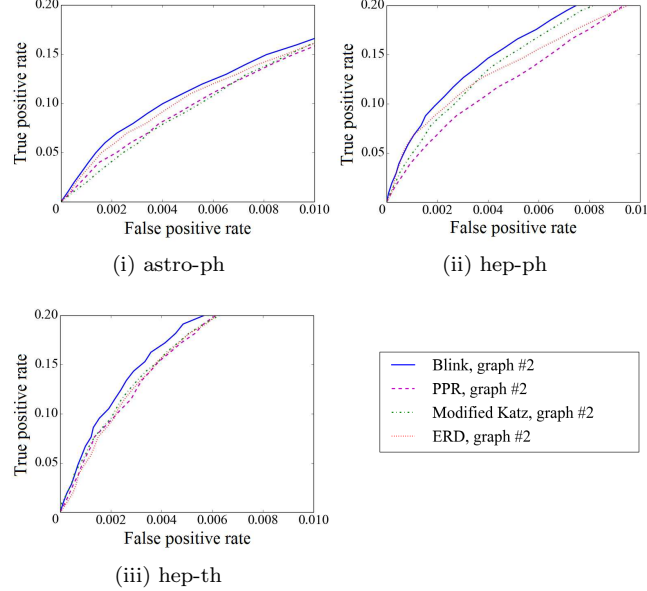


Fig. 4.1: ROC curves on coauthorship networks.

Table 4.3: Statistics of Wikipedia citation networks and prediction tasks.  $n_{\text{page}}$  denotes the number of pages;  $d_{2014}$  and  $d_{2015}$  denote the average number of out-going citations on a 2014/2015 page;  $d_{2014,\text{unique}}$  and  $d_{2015,\text{unique}}$  denote the average number of unique out-going citations on a 2014/2015 page;  $n_{\text{prediction}}$  denotes the average number of additions to predict per task.

	$n_{\text{page}}$	$d_{2014}$	$d_{2014,\text{unique}}$	$d_{2015}$	$d_{2015,\text{unique}}$	$n_{\text{prediction}}$
2014 all pages	4731544	24.66	23.99			
2015 all pages	4964985			24.90	24.23	
qualified tasks	93845	156.1	151.0	162.4	157.0	10.06
training tasks	1000	142.2	137.9	147.5	143.1	10.14
test tasks	1000	159.0	153.3	165.7	159.6	9.85
trimmed test tasks	949	157.6	151.7	164.3	157.9	4.63

**4.2. Link prediction in Wikipedia.** Our second experiment is predicting additions of inter-wikipedia citations in Wikipedia. The rationale is that citation links reflect Wikipedia contributors' perception of relation strength between subjects.

We obtain an inter-wikipedia-citation graph from [11] which was based on Wikipedia dumps generated in April/May 2014, and another graph from [12] which was based on those in February/March 2015. In both graphs, each node represents a Wikipedia page, and each directed edge from node A to node B represents a citation on page A to page B. The ordering of out-going citations from a page A, as they appear in the text on page A, is known and will be utilized by some predictors. Statistics are shown in Table 4.3. 4,631,780 of the 2014 nodes are mapped to 2015 nodes by exact name matching, and another 87,368 are mapped to 2015 nodes by redirection data from [12] which are pages that have been renamed or merged. The remaining 12,396

of the 2014 nodes cannot be mapped: the majority are Wikipedia pages that have been deleted, and some are due to noise in the data collection of [11, 12]. Such noise is a small fraction and has negligible impact to our measurements.

For each mapped node A, we identify  $S_{A,2014}$  as the set of 2014 nodes that page A cites in the 2014 graph and that remain in the 2015 graph,  $S_{A,2015}$  as the set of 2014 nodes that page A cites in the 2015 graph, and  $X_{A,2014}$  as the set of 2014 nodes that cite page A. If page A satisfies the condition that  $5 \leq |(S_{A,2015} \setminus S_{A,2014}) \setminus X_{A,2014}| \leq |S_{A,2014}| \cdot 20\%$ , we consider page A as a qualified prediction task. The rationale behind the size limits is to choose test pages that have undergone thoughtful edits, and their 2014 page contents were already relatively mature; the rationale for excluding in-coming neighbors  $X_{A,2014}$  is to make the tasks more challenging, since simple techniques like heavily weighting in-coming edges have no effect. Statistics are shown in Table 4.3. The number of qualified tasks is large, and we randomly sample a 1000-task training set and a 1000-task test set.

Tasks vary in difficulty. If edits were to make a page more complete, the new links are often reasonably predictable and some are obvious. However, if edits were driven by a recent event, the new links are next to impossible to predict. We form a trimmed test set by removing from the test set targets that are too easy or too difficult, utilizing the outputs of four best-performing predictors on the test set: Adamic/Adar, Blink Model #2, Personalized PageRank #2, and Modified Katz #2. A new link is removed if it ranks less than 20 by all four predictors or if it ranks more than 1000 by all four. The removed prediction targets are excluded from predictor outputs during mean-average-precision evaluation. The results are listed in the last row of Table 4.3 and the last two columns of Table 4.4.

Table 4.4: Comparison of predictor accuracies on additions of inter-wikisite citations in Wikipedia. Each predictor uses its best parameters selected based on the training set.  $R$  denotes the ratio of MAP of a predictor over MAP of Adamic/Adar.

	parameters	training		test		trimmed test	
		MAP	$R$	MAP	$R$	MAP	$R$
Adamic/Adar		0.0291		0.0281		0.0163	
Blink, graph #1	$b_1 = 0.5, b_2 = 0.1$	0.0295	1.014	0.0263	0.937	0.0166	1.019
Blink, graph #2	$b_1 = 0.8, b_2 = 0.8, \gamma = 10$	0.0362	1.244	0.0362	<b>1.289</b>	0.0233	<b>1.428</b>
PPR, graph #1	$\alpha = 0.5$	0.0299	1.029	0.0291	1.038	0.0186	1.140
PPR, graph #2	$\alpha = 0.2, \gamma = 500$	0.0321	1.104	0.0309	1.100	0.0206	1.263
Modified Katz, graph #1	$\beta = 5E-6$	0.0269	0.925	0.0241	0.860	0.0151	0.924
Modified Katz, graph #2	$b_1 = 0.8, b_2 = 0.8, \beta = 0.1, \gamma = 10$	0.0341	1.173	0.0328	1.170	0.0198	1.213
ERD, 100 samples, graph #1	$b_1 = 0.4, b_2 = 0.9$	0.0266	0.914	0.0233	0.830	0.0162	0.996
ERD, 100 samples, graph #2	$b_1 = 0.9, b_2 = 0.9, \gamma = 10$	0.0238	0.817	0.0218	0.778	0.0154	0.944

In Table 4.4, mean average precision (MAP) is the accuracy score. Unlike in Section 4.1, the relations to predict are asymmetric (page A adds a citation to page B) and hence all predictors use their one-directional A-to-B score as is. When multiple node B's have the same score, we use their in-coming degrees as a tie breaker: a node with higher in-coming degree is ranked first. Adamic/Adar is used as a reference, as it represents what can be achieved through good-quality local analysis. In graph #2, we provide domain knowledge through the following  $f_E$  and  $f_V$ . For an edge from node X to node Y and that represents the  $i^{\text{th}}$  citation link on page X:

$$f_E(\text{edge}) = \frac{\delta_{Y,X}}{\max(1, \log_\gamma i) \cdot \max(1, \log_\gamma d_{Y,\text{in}})} \quad (4.1)$$

where  $\delta_{Y,X}$  is 2 if edge exists from Y to X, and 1 otherwise.  $\gamma$  is again a tunable parameter. The above scheme gives higher weight to a citation link if it is located at an earlier location on a page, or if it points to a less-cited page, or if a returning citation exists. Our  $f_V$  function is a direct adaptation of Adamic/Adar's (1.5):  $f_V(\text{node}) = 1/(\log d_{\text{node,in}} + \log d_{\text{node,out}})$ . To get best results, PPR uses (2.7) while Katz and ERD use (2.6). A remarkable observation on Katz with graph #2 is that its best performance happens when (1.3) is almost divergent: with  $b_1 = 0.8$ ,  $b_2 = 0.8$  and  $\gamma = 10$ , the divergence limit for  $\beta$  is 0.1075. For ERD, the reduction in sample numbers from Section 4.1 is because the Wikipedia graph is much larger and denser. Blink Model with graph #2 is clearly the best performer in Table 4.4.

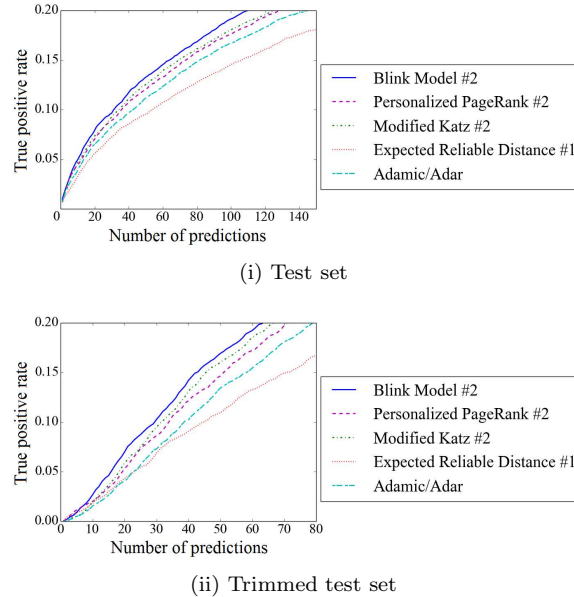


Fig. 4.2: Accuracy curves on Wikipedia citation network.

Figure 4.2 shows a more detailed comparison by plotting true positive rate as a function of the number of predictions made. Blink Model #2 clearly dominates the curves, and for example needs 20 fewer predictions to reach a 20% true positive rate on the test set than the closest competitor.

**5. Conclusions.** This manuscript proposes the Blink Model graph proximity measure. We demonstrate that it matches human intuition better than others, develop an approximation algorithm, and empirically verify its predictive accuracy.

#### REFERENCES

- [1] A. M. Abrahams *et al.*, “Gravitational wave extraction and outer boundary conditions by perturbative matching,” *arXiv:gr-qc/9709082*, 1997.
- [2] L. A. Adamic and E. Adar, “Friends and neighbors on the web,” *Social Networks*, vol. 25, no. 3, pp. 211–230, 2003.
- [3] C. C. Aggarwal, J. L. Wolf, K.-L. Wu, and P. S. Yu, “Horting hatches an egg: A new graph-theoretic approach to collaborative filtering,” in *Proceedings of the ACM SIGKDD International Conference on Knowledge Discovery and Data Mining*, 1999, pp. 201–212.

- [4] M. O. Ball, C. J. Colbourn, and J. S. Provan, “Network reliability,” *Technical Report, University of Maryland*, 1992.
- [5] A.-L. Barabási and R. Albert, “Emergence of scaling in random networks,” *Science*, vol. 286, no. 5439, pp. 509–512, 1999.
- [6] V. D. Blondel, A. Gajardo, M. Heymans, P. Senellart, and P. Van Dooren, “A measure of similarity between graph vertices: Applications to synonym extraction and web searching,” *SIAM Review*, vol. 46, no. 4, pp. 647–666, 2004.
- [7] B. Bollobas and O. Riordan, *Percolation*. Cambridge University Press, 2006.
- [8] T. B. Brecht and C. J. Colbourn, “Lower bounds on two-terminal network reliability,” *Discrete Applied Mathematics*, vol. 21, no. 3, pp. 185–198, 1988.
- [9] P. Y. Chebotarev and E. V. Shamis, “Matrix-forest theorem and measuring relations in small social groups,” *Automation and Remote Control*, vol. 58, no. 9, pp. 1505–1514, 1997.
- [10] W. Chen, L. V. Lakshmanan, and C. Castillo, *Information and Influence Propagation in Social Networks*. Morgan & Claypool, 2013.
- [11] DBpedia, “DBpedia 2014 Downloads,” 2014, [Available at <http://wiki.dbpedia.org/Downloads2014>; accessed 22-April-2015].
- [12] —, “DBpedia Downloads 2015-04,” 2015, [Available at <http://wiki.dbpedia.org/Downloads2015-04>; accessed 20-August-2015].
- [13] P. Erdos and A. Renyi, “On random graphs I.” *Publicationes Mathematicae Debrecen*, vol. 6, pp. 290–297, 1959.
- [14] C. Faloutsos *et al.*, “Fast discovery of connection subgraphs,” in *Proceedings of the ACM SIGKDD International Conference on Knowledge Discovery and Data Mining*, 2004, pp. 118–127.
- [15] G. S. Fishman, “A comparison of four monte carlo methods for estimating the probability of s-t connectedness,” *IEEE Transactions on Reliability*, vol. 35, no. 2, pp. 145–155, 1986.
- [16] F. Fouss, A. Pirotte, J.-M. Renders, and M. Saerens, “Random-walk computation of similarities between nodes of a graph with application to collaborative recommendation,” *IEEE Transactions on Knowledge and Data Engineering*, vol. 19, no. 3, pp. 355–369, 2007.
- [17] E. N. Gilbert, “Random graphs,” *The Annals of Mathematical Statistics*, vol. 30, no. 4, pp. 1141–1144, 1959.
- [18] G. Hardy, C. Lucet, and N. Limnios, “K-terminal network reliability measures with binary decision diagrams,” *IEEE Transactions on Reliability*, vol. 56, no. 3, pp. 506–515, 2007.
- [19] P. Jaccard, “The distribution of the flora in the alpine zone,” *New Phytologist*, vol. 11, no. 2, pp. 37–50, 1912.
- [20] G. Jeh and J. Widom, “Simrank: a measure of structural context similarity,” in *Proceedings of the ACM SIGKDD International Conference on Knowledge Discovery and Data Mining*, 2002, pp. 538–543.
- [21] R. Jin, L. Liu, B. Ding, and H. Wang, “Distance-constraint reachability computation in uncertain graphs,” *Proceedings of the VLDB Endowment*, vol. 4, no. 9, pp. 551–562, 2011.
- [22] D. R. Karger, “A randomized fully polynomial time approximation scheme for the all-terminal network reliability problem,” *SIAM Review*, vol. 43, no. 3, pp. 499–522, 2001.
- [23] L. Katz, “A new status index derived from sociometric analysis,” *Psychometrika*, vol. 18, no. 1, pp. 39–43, 1953.
- [24] D. Kempe, J. Kleinberg, and É. Tardos, “Maximizing the spread of influence in a social network,” in *Proceedings of the ACM SIGKDD International Conference on Knowledge Discovery and Data Mining*, 2003, pp. 137–146.
- [25] H. Kesten, *Percolation Theory for Mathematicians*. Springer, 1982.
- [26] Y. Koren *et al.*, “Measuring and extracting proximity in networks,” in *Proceedings of the ACM SIGKDD International Conference on Knowledge Discovery and Data Mining*, 2006, pp. 245–255.
- [27] N. Lao and W. W. Cohen, “Relational retrieval using a combination of path-constrained random walks,” *Machine Learning*, vol. 81, no. 1, pp. 53–67, 2010.
- [28] E. Leicht, P. Holme, and M. E. Newman, “Vertex similarity in networks,” *Physical Review E*, vol. 73, no. 2, p. 026120, 2006.
- [29] D. Liben-Nowell and J. Kleinberg, “The link-prediction problem for social networks,” *Journal of the American Society for Information Science and Technology*, vol. 58, no. 7, pp. 1019–1031, 2007.
- [30] R. N. Lichtenwalter, J. T. Lussier, and N. V. Chawla, “New perspectives and methods in link prediction,” in *Proceedings of the ACM SIGKDD International Conference on Knowledge Discovery and Data Mining*, 2010, pp. 243–252.
- [31] W. Liu and L. Lü, “Link prediction based on local random walk,” *Europhysics Letters*, vol. 89, no. 5, p. 58007, 2010.

- [32] M. Nickel, K. Murphy, V. Tresp, and E. Gabrilovich, “A review of relational machine learning for knowledge graphs: From multi-relational link prediction to automated knowledge graph construction,” *Center for Brains, Minds, Machines Memo 028*, 2015.
- [33] L. Page, S. Brin, R. Motwani, and T. Winograd, “The pagerank citation ranking: bringing order to the web,” *Technical Report, Stanford University*, 1999.
- [34] T. Politof and A. Satyanarayana, “Efficient algorithms for reliability analysis of planar networks: a survey,” *IEEE Transactions on Reliability*, vol. 35, no. 3, pp. 252–259, 1986.
- [35] M. Potamias, F. Bonchi, A. Gionis, and G. Kollios, “K-nearest neighbors in uncertain graphs,” *Proceedings of the VLDB Endowment*, vol. 3, no. 1, pp. 997–1008, 2010.
- [36] H. Qian, “Link prediction benchmarks,” 2016, [Available at <http://researcher.watson.ibm.com/group/6672>].
- [37] H. Qian and H. Wan, “Ranking related objects using blink model based relation strength determinations,” *U.S. Patent Application 14/791789*, 2015.
- [38] J. E. Ramirez-Marquez and D. W. Coit, “A monte-carlo simulation approach for approximating multi-state two-terminal reliability,” *Reliability Engineering & System Safety*, vol. 87, no. 2, pp. 253–264, 2005.
- [39] A. Satyanarayana and R. K. Wood, “A linear-time algorithm for computing k-terminal reliability in series-parallel networks,” *SIAM Journal on Computing*, vol. 14, no. 4, pp. 818–832, 1985.
- [40] H. Tong *et al.*, “Fast direction-aware proximity for graph mining,” in *Proceedings of the ACM SIGKDD International Conference on Knowledge Discovery and Data Mining*, 2007, pp. 747–756.
- [41] L. G. Valiant, “The complexity of enumeration and reliability problems,” *SIAM Journal on Computing*, vol. 8, no. 3, pp. 410–421, 1979.
- [42] R. Van Slyke and H. Frank, “Network reliability analysis: Part I,” *Networks*, vol. 1, no. 3, pp. 279–290, 1971.
- [43] C. Wang, W. Chen, and Y. Wang, “Scalable influence maximization for independent cascade model in large-scale social networks,” *Data Mining and Knowledge Discovery*, vol. 25, no. 3, pp. 545–576, 2012.
- [44] L. Yen *et al.*, “A family of dissimilarity measures between nodes generalizing both the shortest-path and the commute-time distances,” in *Proceedings of the ACM SIGKDD International Conference on Knowledge Discovery and Data Mining*, 2008, pp. 785–793.
- [45] Y. Yuan, L. Chen, and G. Wang, “Efficiently answering probability threshold-based shortest path queries over uncertain graphs,” in *International Conference on Database Systems for Advanced Applications*, 2010, pp. 155–170.
- [46] Z. Zou, J. Li, H. Gao, and S. Zhang, “Mining frequent subgraph patterns from uncertain graph data,” *IEEE Transactions on Knowledge and Data Engineering*, vol. 22, no. 9, pp. 1203–1218, 2010.